American Mineralogist, Volume 77, pages 647–655, 1992

Improvements of the Shaw membrane technique for measurement and control of f_{H_2} at high temperatures and pressures

Bruno Scaillet,* Michel Pichavant*

Centre de Recherches sur la Synthèse et la Chimie des Minéraux, CNRS, 1A rue de la Férollerie, 45071 Orléans, France and Centre de Recherches Pétrographique et Géochimiques, CNRS, B.P. 20, 54501, Vandoeuvre-lès-Nancy, France

Jacques Roux, Georges Humbert, André Lefèvre

Centre de Recherches sur la Synthèse et la Chimie des Minéraux, CNRS, 1A rue de la Férollerie, 45071 Orléans, France

Abstract

The lifetimes of fayalite + magnetite + quartz and cobalt + cobalt oxide O buffers have been determined in sealed Au capsules at high temperatures (>700 °C) in Ar-pressurized vessels. At 750 °C and 4500 bars, lifetimes are <60 h and <155 h for 100 mg of fayalite and cobalt, respectively, in the starting buffer assemblage. For hydrothermal experiments longer than a few days under moderately reducing conditions, the Shaw membrane is the only working technique for measurement and control of f_{H_2} at high temperatures and pressures. Different membranes have been constructed and systematically tested under various conditions (e.g., different types of pressure vessel, temperatures, total pressures and gas mixtures), and the results are compared to calculated H_2 mass transfers. For cold-seal pressure vessels (CSPV) fitted with Pt membranes, the type of membrane response is identical to that described by Hewitt (1978) and well modeled by calculations (in both membrane and vessel). Osmotic equilibrium between membrane and vessel can be attained after about 2 d but cannot be maintained for longer than a few hours because of H_2 loss through the vessel walls. In contrast, for internally heated pressure vessels (IHPV) fitted with AgPd membranes, osmotic equilibrium is attained after about 2 h and maintained, in spite of some H_2 loss through the vessel walls. The good agreement between observed and calculated f_{H_2} supports the validity of the experimental data base for H_2 permeability in noble metals and steels.

We also present a new membrane design for use in an IHPV. With this design, H_2 diffusion is limited to the reaction zone, as confirmed by use of the H_2 sensors of Chou and Eugster (1976). Use of a Au cell together with this new membrane allows partial confinement of H_2, thus enabling accurate control and measurement of f_{H_2} in IHPV. In addition, this procedure limits potential hazards due to interactions of H_2 with autoclave steels. This study also stresses the importance of measuring volumes of the vessel and membrane in determining the f_{H_2} regime. In practice, the use of low-permeability membranes such as Pt in CSPV should be avoided.

Introduction

There are presently only two techniques available for controlling the f_{H_2} and f_{O_2} under hydrothermal P-T conditions: the double-capsule technique (Eugster, 1957, 1959) and the Shaw membrane (Shaw, 1963). Both of these methods are based on the permeability of H_2 in precious metals or alloys (typically Pt and AgPd), which are used as containers in the experiments. Because of its simplicity, the double-capsule technique has been widely adopted while the Shaw membrane is less popular, probably because of the need for more sophisticated apparatus.

We have tested these two techniques in an experimental program designed to establish the phase equilibrium relations of felsic peraluminous granitic rocks (Scaillet et al., 1991). The double-capsule technique was first employed and soon demonstrated to be unsuitable. For example, f_{H_2} values corresponding to fayalite + magnetite + quartz (FMQ) and cobalt + cobalt oxide (CCO) could not be maintained for long times at 750 °C and 4.5 kbar in an internally heated pressure vessel (IHPV) pressurized with Ar because of the very rapid exhaustion of fayalite and cobalt, irrespective of the thickness of the Au capsule (Hamilton et al., 1964). For hydrothermal experiments longer than a few days under moderately reducing conditions, the Shaw membrane is the only working technique for measurement and control of f_{H_2} at high temperatures and pressures. Unfortunately, there are few

* Present address: Centre de Recherches sur la Synthèse et la Chimie des Minéraux, CNRS, 1A rue de la Férollerie, 45071 Orléans, France.

0003–004X/92/0506–0647$02.00

TABLE 1. Experimental and calculated lifetime of QFM and CCO solid buffers in IHPV at around 750 °C, 4500 bars

Buffer	Fe_2SiO_4-Fe_3O_4-SiO_2 (FMQ) (log f_{O_2}* = −15.36 atm, f_{H_2}** = 29.4 bars)			Co-CoO (CCO) (log f_{O_2}† = −16.26 atm, f_{H_2}** = 82.2 bars)	
Experiment no.	1	2	3	4	5
Mass of reduced assemblage in the starting product (mg)‡	98.5	49.5	100.3	108.9	95.2
Experiment duration (h)	157	264	157	157	20
Capsule thickness (mm)	0.4	0.4	0.8	0.4	0.8
Experimental products	Q, M	Q, M	Q, M	CO	C, CO
Maximum buffer lifetime, calculated (h)§	30.2	15.2	57.5	95.0	155.3
Mass of reduced assemblage oxidized, calculated (mg)§	512.3	861.5	273.9	180	12.3

Note: Q = quartz; M = magnetite; C = cobalt; CO = CoO.

* Calculated from Hewitt (1978), in Chou (1987).

** Calculated using f_{H_2} coefficients (Shaw and Wones, 1964), interpolated f_{H_2O} (Burnham et al., 1969) and interpolated H_2O dissociation constants (Robie et al., 1978).

† Calculated from Chou (1978), in Chou (1987).

‡ Loaded with an amount of H_2O sufficient for complete oxidation.

§ Calculated from Equation 1, permeability data for Au taken from Chou (1986), r_e = 2.9 mm or 3.3 mm, r_i = 2.5 mm, l = 30 mm, $f^{i}_{H_2}$ = 29.4 bars (FMQ) or 82.2 bars (CCO) and $f^{e}_{H_2}$ = 1 bar. See text and Figure 1 for additional details.

published works describing the practical use of such membranes. Hewitt (1978), Gunter et al. (1979), and Frantz et al. (1977) provided information on membrane construction and kinetics of equilibration for cold-seal pressure vessels (CSPV). Piwinskii et al. (1973) presented a design of an osmotic membrane for IHPV. In this paper, we present systematic tests of the use of Shaw membranes under various conditions (different types of pressure vessel, temperatures, total pressures and gas mixtures). Different types of Shaw membranes, including a new membrane for an IHPV whose design is described below, have been constructed and compared. We also show the results of our calculations of H_2 mass transfer that allow modeling of kinetics of membrane equilibration and comparison with the experimental data.

LIFETIME OF FMQ AND CCO O BUFFERS AND RESTRICTION OF THE USE OF THE SOLID BUFFER METHOD

Experimental tests were performed to determine the lifetime of the FMQ (fayalite + magnetite + quartz) and CCO (cobalt + cobalt oxide) buffers at around 750 °C and 4.5 kbar. These two buffer assemblages yield similar f_{O_2} values [log f_{O_2} (FMQ) − log f_{O_2} (CCO) = 0.67 at 1 bar and 700 °C] (buffer equations of Hewitt, 1978, for QFM; and Chou, 1978, for CCO, listed in Chou, 1987), yet their buffering capacities differ markedly (Chou, 1987). The experiments consisted of running the two solid buffers in sealed Au capsules of various thicknesses in a large volume IHPV pressurized with Ar. The ambient f_{H_2} of this vessel has been experimentally bracketed between nickel + nickel oxide (NNO) and manganosite + hausmannite (MnO + Mn_3O_4), in agreement with previous determinations for IHPV (Chou, 1978). Different masses of the reduced assemblages and different experiment durations were tested. The quantity of added H_2O was in all cases sufficient for complete oxidation of the reduced assemblage. Fayalite was synthesized after Hewitt (1978). CoO was synthetized from Co in a 1-atm gas-mixing furnace at T = 1100 °C and log f_{O_2} = −8.45. The progressive exhaustion of the reduced assemblage in the experiments was determined by X-ray diffraction techniques (CCO and FMQ) and optical examination (quartz + magnetite overgrowths on fayalite). Results of these experiments are shown in Table 1. Total oxidation of the reduced assemblages (50–100 mg) was observed in all experiments longer than 6 d. This results from H_2 loss through the capsule walls caused by a gradient in f_{H_2} between the capsule and the vessel. Under these experimental conditions in this apparatus, even increasing the Au capsule thickness up to 0.8 mm does not greatly reduce the H_2 loss (Table 1). These experimental data were complemented by the calculation of the masses of fayalite and Co being oxidized under these conditions (see below, Fig. 1 and Table 1 for information on these calculations). The results show that, for masses of reduced assemblages in the range of 50–100 mg, buffer lifetimes are in the range 0.6–2.4 d for FMQ and 4–6.5 d for CCO. For experiments of several weeks at QFM or CCO in IHPV pressurized with Ar, hundreds of milligrams to several grams of the reduced assemblage appear to be required to counteract only the H_2 loss (Table 1 and Fig. 1). This is a serious limitation to the use of the solid buffer technique at high temperature in gas (Ar, N_2) pressure vessels. In addition, there are known to be specific problems with some buffers, such as QFM (steady-state f_{H_2} levels lower than equilibrium values, Chou and Cygan, 1989; small buffering capacity, Chou, 1987), and this constitutes an additional restriction on the use of the solid buffer method.

PRACTICAL AND THEORETICAL USE OF SHAW MEMBRANES

Membrane design and construction

The membranes used in the CSPV are based on the design of Hewitt (1978). These were made of Pt (thickness 0.2 mm, id 2.5 mm, length 40 mm) filled with rounded quartz grains (natural sand, grain size 0.5 mm).

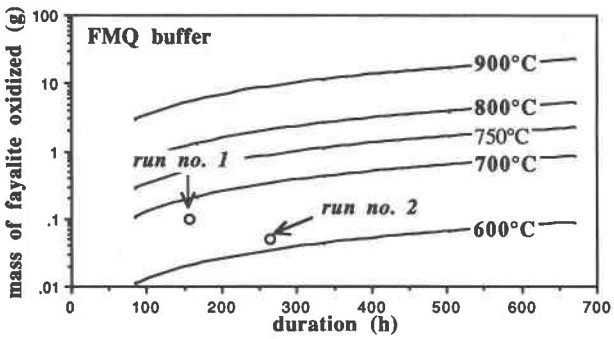

Fig. 1. Calculations of the mass of fayalite oxidized (g) in FMQ buffer assemblages as a function of experiment duration (h) and temperature (600–900 °C) at 4500 bars for vessels pressurized with Ar. Fayalite (together with quartz and magnetite) is contained in a Au capsule 30 mm long with an inner diameter of 5 mm and a thickness of 0.4 mm. H_2 loss through the capsule walls is modeled by Equation 1 (Harvie et al., 1980). See Table 1 for details of the calculations. The lines drawn represent masses of fayalite oxidized to quartz and magnetite as a function of experiment duration and for different temperatures. Also plotted for illustration are the experimental conditions of experiments 1 and 2 (see Table 1). The experimental points are located below the 750 °C isotherm, which indicates that all fayalite of the buffer assemblage must have been oxidized. For conditions of experiment 2 (750 °C, 264 h, Table 1), a mass of fayalite of about 1 g in the buffer assemblage is needed to prevent total exhaustion by oxidation.

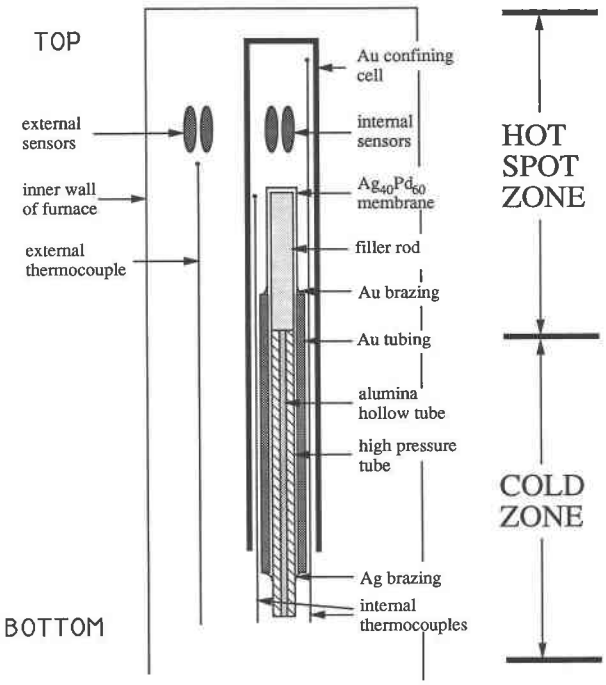

Fig. 2. Schematic diagram of the new membrane design used in this study for IHPV (not drawn to scale). For clarity, all the pieces of the assembly have been slightly spread (see details in text).

The membrane was brazed (Hewitt, 1978) on a Au-plated stainless-steel high-pressure capillary.

For the IHPV, a new membrane configuration was designed (Fig. 2). The membranes were made of either Pt or $Ag_{40}Pd_{60}$. These were in all cases filled with a solid rod of AlSiMag (od 5 mm). A stainless-steel high-pressure tube (od 5 mm, id 1.8 mm) filled with a hollow alumina tube (od 1.8 mm, id 0.2 mm) was placed inside a Au tube (od 6.6 mm, id 5 mm, length 100 mm) and Ag brazed at its bottom end. The membrane (od 5.4 mm, id 5 mm, length 40 mm) and filling rod were inserted at the top end of the Au tube and Au brazed (Fig. 2). With this design, the H_2 diffusing zone is limited to the hot spot where the temperature can be accurately determined (Roux and Lefèvre, 1992), and problems due to collapse of the high-pressure capillary at high P and T are eliminated.

For some experiments in IHPV, a confining cell welded at its top end was placed around the membrane (Fig. 2). In theory, this cell should reduce the volume of the H_2 reservoir and therefore the time of equilibration between the membrane and the vessel. This is a principle already employed by Frantz et al. (1977) in CSPV. However, in our case the tube was not soldered to the membrane (Frantz et al., 1977) but was left open to the cold part of the furnace (<100 °C, Fig. 2). This new configuration makes it possible to control f_{H_2} in IHPV without using H_2-Ar mixtures as the initial pressurizing media, thus reducing potential problems caused by H_2 embrittlement of autoclave steels (Seward and Kishima, 1987). Au was the metal chosen for the confining tube because of its low permeability to H_2 (Chou, 1986). The efficacy of this Au confining tube has been tested and the results will be given later.

Experimental apparatus

The osmotic equilibrium experiments were performed in two kinds of hydrothermal vessels: a cold-seal vessel (free volume = 4 cm^3) made of René-41 alloy held horizontally and an internally heated pressure vessel (free volume = 414 cm^3) made of an alloy similar to that used by Holloway (1971), held vertically. The CSPV was calibrated under pressure by using a sheathed dual chromel-alumel thermocouple (Pichavant, 1987). Temperatures during the experiment were measured by an external unsheathed chromel-alumel thermocouple and were recorded continuously. The thermocouples were calibrated against the melting of NaCl at 1 bar, and the overall maximum error on temperature is ±10 °C. Temperatures in the IHPV were measured with three unsheathed and two sheathed chromel-alumel thermocouples calibrated against NaCl melting at 1 bar and 2 kbar. The furnace of the IHPV allows a hot-spot zone of 8 cm in length and 2.3 cm in diameter, with a thermal gradient less than 2 °C across (Roux and Lefèvre, 1992). The intrinsic f_{H_2} of this IHPV is less than 1 bar (see below).

For all experiments the pressure medium was either pure Ar or H_2, or mixtures of these two gases. Total pres-

sures were measured with transducers calibrated against Heise Bourdon tube gauges (error ± 0.020 kbar). H_2 pressures were measured with Protais tube gauges (uncertainty of about 0.1 bar). The total volume of the H_2 line (including the membrane) ranges between 11 and 17 cm^3, depending on the gauge used.

Calculations

Theoretical mass transfer of H_2 (grams of H_2, M_{H_2}) through the membrane or capsule was calculated from the equation of Harvie et al. (1980):

$$\frac{dM_{H_2}}{dt} = \frac{2\pi kl}{\ln\left(\frac{r_e}{r_i}\right)}\left(\sqrt{f^i_{H_2}} - \sqrt{f^e_{H_2}}\right) \quad (1)$$

where k is the permeability constant of H_2, l is the length of the membrane or capsule, r_e and r_i are the external and internal radii of the membrane or capsule, and $f^i_{H_2}$ and $f^e_{H_2}$ the internal (membrane or capsule) and external (vessel) f_{H_2}. The value of k is taken from Chou (1986) for Au and Pt and from Gunter et al. (1987) for AgPd alloys, steels, and vessel alloys. The volumes of the different H_2 reservoirs (H_2 line, capsule, vessel) are given above.

Two types of calculations have been carried out. First, the above equation was employed to calculate the mass of fayalite exhausted by oxidation in FMQ assemblages (see above, Fig. 1 and Table 1). In this case, $f^i_{H_2}$ is that fixed by the FMQ and CCO buffer and $f^e_{H_2}$ is assumed to be 1 bar. Because of the negligible volume of the capsule compared to the IHPV, $f^i_{H_2} - f^e_{H_2}$ is constant in these calculations. For a given duration (dt, Fig. 1), the equation gives the mass of H_2 transferred from the capsule, which is then converted to a mass of fayalite (Fig. 1) according to the reaction

$$\tfrac{3}{2}\,Fe_2SiO_4 + H_2O = Fe_3O_4 + \tfrac{3}{2}\,SiO_2 + H_2.$$

Second, the evolution with time of H_2 pressures in both the membrane and vessel was calculated in order to allow comparison with experimental data. In this case, $f^i_{H_2} - f^e_{H_2}$ is no longer constant, and the calculations must follow an iterative procedure. For a given $f^i_{H_2}$ and $f^e_{H_2}$ couple, corresponding to $M^i_{H_2}$ and $M^e_{H_2}$, respectively, the amount of H_2 transferred through the membrane during dt is calculated. This generates new $M^i_{H_2}$ and $M^e_{H_2}$ values, which are used to calculate a new set of $f^i_{H_2}$ and $f^e_{H_2}$. The main assumptions made in these calculations are the following:

1. Values of f_{H_2} are calculated from M_{H_2} assuming ideal mixing of perfect gases (Ar and H_2).

2. The intrinsic f_{H_2} of the vessels is assumed to be zero (i.e., $f^e_{H_2} = 0$). Although this is not exactly true for our IHPVs (see above), this is a convenient approximation that does not significantly affect the final result.

3. The free volume of the vessel (external H_2 reservoir) is assumed to be at a uniform temperature determined by the experimental conditions.

4. Results for the CSPV take into account the loss of H_2 through the vessel walls, which is calculated in the same manner as for the membrane. In contrast, calculations for the IHPV assume no loss of H_2 in the vessel walls.

5. For metal membranes having high permeabilities such as $Ag_{40}Pd_{60}$, the integration parameter (dt) is a function of the magnitude of the difference between $f^i_{H_2}$ and $f^e_{H_2}$.

Experimental procedure and results

Three experimental procedures were studied at 600 °C and various total pressures (P_{tot} = 100–4500 bars) in a CSPV fitted with Pt membranes. In procedure 1, the CSPV was loaded at room temperature with a known pressure of pure H_2 (53 bars). The temperature was brought to the desired value, and both the vessel pressure (in this case $P_{tot} = P_{H_2}$) and membrane pressure were recorded. A typical response of the system under these conditions is shown in Figure 3. The membrane pressure (starting from an initially applied pressure of 6 bars) first rises because of H_2 diffusion from the vessel, then reaches a maximum of about 8.6 bars after 52 h, and then slowly decreases at a rate of about 10^{-2} bars/h (Fig. 3B). In contrast, the vessel pressure, after an initial rapid rise on heating (up to around 100 bars), decreases rapidly and continuously (Fig. 3A). Equilibrium between vessel and membrane H_2 pressures is attained after 52 h and corresponds to the maximum pressure recorded by the membrane. For longer durations, the vessel pressure continues to drop because of H_2 loss through the walls (Fig. 3A). Because the volume of the vessel is smaller than that of the membrane, the decrease of H_2 pressure is more pronounced in the vessel than in the membrane (Fig. 3A). Figure 3B shows observed and calculated P_{H_2} in the membrane for different values of log k for the vessel. A satisfactory fit between observed and calculated membrane P_{H_2} is obtained for log $k = -9.8$ mol H_2/cm·s·bar$^{1/2}$ which compares well with that given by Gunter et al. (1987) for Nichrom (log $k = -9.76$ H_2/cm·s·bar$^{1/2}$). Therefore, a value of log $k = -9.8$ H_2/cm·s·bar$^{1/2}$ is retained for further calculations in CSPV.

In procedure 2, the vessel was loaded at room temperature with ~850 bars of Ar and the membrane was loaded with 3.85 bars of H_2. The vessel was then brought to 600 °C corresponding to 1000 bars of Ar. Figure 4A shows the membrane response, which is characterized by a continuous drop of H_2 pressure. In contrast to the previous case, the rate of decreasing H_2 pressures changes with time, from an initially high value of 10^{-1} bars/h down to 10^{-3} bars/h after 100 h. This results from the coupled effects of (1) faster H_2 permeabilities in Pt than in vessel alloy (Gunter et al., 1987) and (2) the greater volume of the H_2 line (membrane) compared with that of the vessel. Predicted H_2 pressures agree with observed pressures within less than 0.5 bars (Fig. 4A).

In the last procedure, 3, the CSPV was loaded at room temperature with H_2 (45 bars), Ar was added to a total

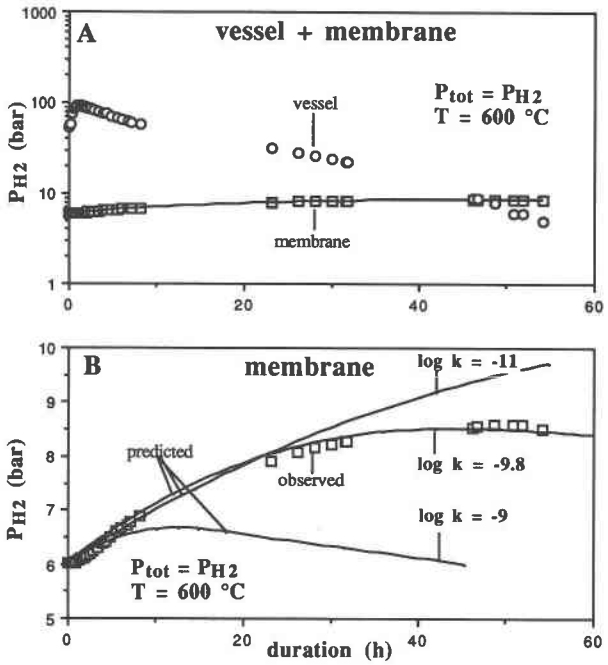

Fig. 3. P_{H_2} vs. experiment duration for a CSPV equipped with a Pt membrane and using pure H_2 as pressure medium. (**A**) Evolution of P_{H_2} in the two H_2 reservoirs (membrane and vessel). (**B**) Same experiment showing comparison between observed (open squares) and calculated membrane P_{H_2} (lines) for different values of log k for the vessel alloy. Note the difference in vertical scale between **A** and **B**.

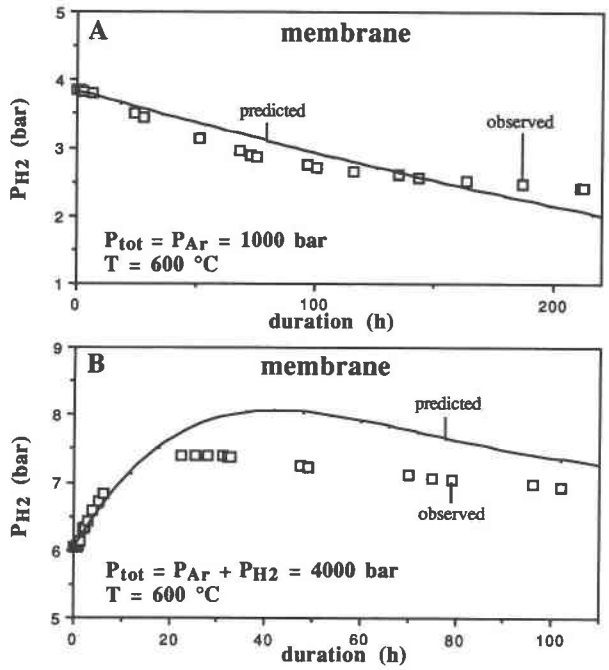

Fig. 4. Observed and predicted P_{H_2} in Pt membrane vs. experiment duration for a CSPV. (**A**) Vessel loaded with Ar (see text). (**B**) Vessel loaded with a mixture of Ar and H_2 (see text). Same symbols as in Figure 3.

pressure of 2260 bars, and then the temperature was brought to the desired value. The response of the membrane at a total pressure of $P_{Ar} + P_{H_2} = 4000$ bars at 600 °C (Fig. 4B) is similar to that observed with pure H_2 (Fig. 3B), although the maximum H_2 pressure (7.4 bars), is here reached after about 28 h. The maximum in P_{H_2} is followed by a continuous decrease of the H_2 pressure at the same rate as with pure H_2 (10^{-2} bars/h). Calculations yield H_2 pressures in good agreement with the observed values for durations of less than 20 h. From then on, the predicted H_2 pressures are consistently higher than the measured pressures by about 0.8 bars, and the maximum predicted H_2 pressure occurs at ~50 h (Fig. 4B). Although the cause of this discrepancy is not totally clear, it is possible that some of our assumptions (perfect gas behavior of H_2 and the temperature distribution within the vessel) are not entirely valid at high pressures for Ar-H_2 mixtures. Furthermore, high pressures may affect the mechanisms of diffusion of H_2 in both autoclave steels and metal membranes (Gunter et al., 1987; Chou and Cygan, 1989). Nevertheless, our calculations performed in the 100–4500 bar range use permeability constants (log k) that have been determined at ≤1 bar for Nichrom (Gunter et al., 1987) and at 2 kbar for noble metal membranes (Chou, 1986) only. In addition, the mechanisms of diffusion of H_2 in noble metals, hence permeability constants, may also depend on the pressure medium (Chou and Cygan, 1990).

Experiments in IHPV were performed at 4000 bars in the 700–750 °C range, with Pt and $Ag_{40}Pd_{60}$ membranes. Two experimental procedures were tested, differing in the method of introducing H_2. Procedure 1, similar to procedure 3 described above for the CSPV, consisted of loading the vessel with a mixture of Ar and H_2 so that f_{H_2} were about 5 times higher than in CSPV. The results of membrane response for $Ag_{40}Pd_{60}$ (Fig. 5) show no major difference with data acquired in CSPV (Figs. 3B, 4B). However, H_2 pressures rise faster in AgPd than in Pt

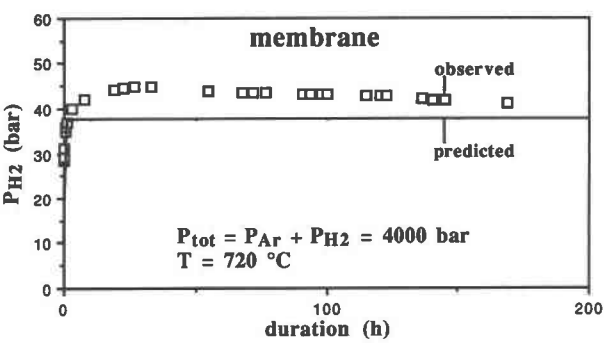

Fig. 5. Observed and predicted P_{H_2} membrane vs. experiment duration for an IHPV equipped with an $Ag_{40}Pd_{60}$ membrane. Vessel loaded with a mixture of Ar and H_2 (see text). Same symbols as in Figure 3. Note the significant difference between observed and calculated P_{H_2} values.

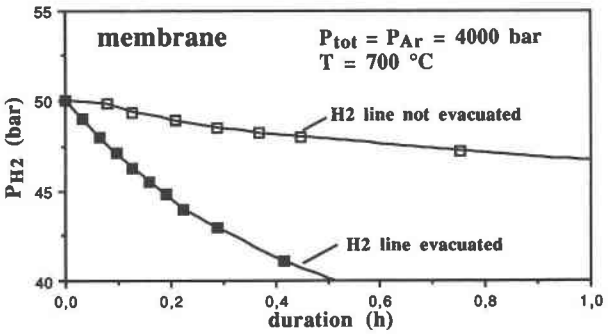

Fig. 6. Effect of air trapped in the H_2 line for an IHPV equipped with an $Ag_{40}Pd_{60}$ membrane. Vessel loaded with pure Ar (see text). The lines of decreasing P_{H_2} membrane vs. experiment duration indicates diffusive transfer of H_2 from the membrane toward the vessel. Note the fast drop of P_{H_2} membrane when the H_2 line has been previously air evacuated.

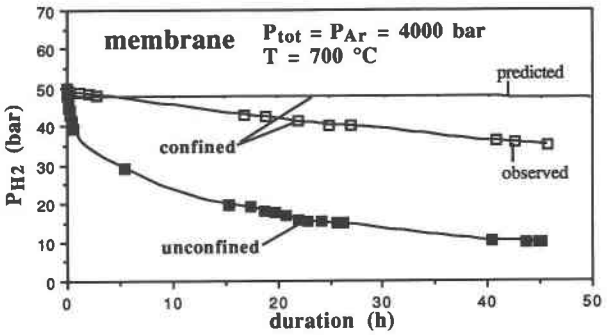

Fig. 7. Effect of the Au confining cell on the rate of H_2 transfer from the membrane into the IHPV. Same conditions as in Figure 6 and H_2 line evacuated. Note the important slowing of the H_2 transfer from the membrane into the vessel with the confining cell present.

membranes (compare Fig. 5 with Figs. 3B and 4B), and the maximum H_2 pressure (from an initial H_2 pressure of 9 bars) is attained more rapidly in the AgPd membrane (45 bars, 25 h; Fig. 5). As in the CSPV experiment, the membrane H_2 pressure then decreases continuously at the constant rate of $3 \cdot 10^{-2}$ bars/h (Fig. 5). Calculated membrane responses (Fig. 5), however, show more substantial disagreement with experimental data. This indicates more difficulty in predicting the H_2 behavior in IHPV than in CSPV. Our assumptions of uniform temperature of the vessel free volume and of no H_2 loss through the vessel walls are likely to be in error for IHPV. The observed decrease in H_2 pressures (Fig. 5) is considered a positive indication of H_2 diffusing into the vessel walls.

In procedure 2, only Ar was pumped into the vessel. The H_2 line and the AgPd membrane were pressurized to a known value of P_{H_2} (always 50 bars), and the transfer of H_2 from the membrane into the vessel was studied. We observed that the kinetics of H_2 transfer was significantly dependent on the presence or absence of trapped air in the H_2 line (Fig. 6). With a previously air-evacuated H_2 line, a relatively fast H_2 transfer from the membrane toward the vessel is apparent from the rapid decrease of the membrane P_{H_2} with time, starting from the initially applied value of 50 bar P_{H_2} (Fig. 6). Such a transfer is slowed substantially when air is present (Fig. 6), suggesting a poor mixing among gases in the H_2 line and some type of plugging effect of air. In all experiments described below, the H_2 line was therefore systematically air evacuated for at least 15 min prior to introducing H_2.

Figure 7 shows the effect of using a Au confining cell (Fig. 2). Without the cell, the initially rapid decrease of the membrane P_{H_2} (Figs. 6, 7) progressively flattens (Fig. 7) and reaches about 10 bars for 40 h. For longer durations (not shown on Fig. 7), P_{H_2} falls below 1 bar, thus approaching the intrinsic f_{H_2} of the vessel (see above). In comparison, the presence of the confining cell causes an important damping effect on the transfer of H_2 toward the vessel, maintaining P_{H_2} values close to 50 bars for significant durations. The calculated membrane response is essentially flat after an initial stage of rapidly decreasing P_{H_2}, corresponding to the infilling of the cell free volume (3 cm^3) by H_2 (Fig. 7). Unfortunately, our calculations do not exactly reproduce the experimental data, since total pressures must equilibrate between the inside and the outside of the cell. Thus some loss of H_2 at the bottom end of the cell is probably unavoidable with the rather loose closure system adopted here for the cell (Fig. 2). In spite of this shortcoming, the data obtained (Fig. 7) show that this experimental configuration is useful for practical purposes.

An independent check for the P_{H_2} values read by the membrane was obtained by using the H_2 sensor technique (Chou and Eugster, 1976; Chou, 1987). This test was carried out in IHPV and with the same experimental configuration as above (i.e., Au confining cell present, Fig. 2). The results are presented in Table 2. Good agreement is obtained among the membrane and the two sensors placed inside the confining cell (35 and an average of 41 bars, respectively) indicating that the membrane indeed records the P_{H_2} prevailing inside the cell. However, it is worth noting that the sensors give no information on the evolution of P_{H_2} with time; only the final P_{H_2} value is measured (compare Fig. 7 and Table 2). These data also support the previous experimental tests of Frantz et al. (1977) concerning the reliability of the H_2 sensor technique. Conversely, the sensors placed outside the cell yield P_{H_2} values (average of 7 bars) that are much lower than those of the other sensors. This is a value substantially higher than the intrinsic P_{H_2} of the vessel (<1 bar), demonstrating that our experimental configuration does not totally prevent H_2 loss from inside the confining cell (see above).

Discussion and Conclusions

Several improvements of the Shaw membrane technique have been presented in this paper, mainly for use in IHPV, and these are discussed in detail below. First, a new membrane design has been proposed and success-

TABLE 2. Comparison of the Shaw membrane and H_2 sensor technique (Chou, 1987) at 700 °C and 4000 bars

	MCl^{-}* (mol/L)	mCl^{-} (mol/kg)	P_{H_2}** (bars)	log f_{O_2}†	ΔFMQ‡
Membrane (inside the confining cell)	—	—	35§	−17.03	−0.38
Sensor A (inside the confining cell)	0.847	0.862	40.7	−17.17	−0.52
Sensor B (inside the confining cell)	0.852	0.867	41.2	−17.18	−0.53
Sensor A (outside the confining cell)	0.343	0.346	6.6	−15.58	+1.07
Sensor B (outside the confining cell)	0.363	0.366	7.3	−15.66	+0.99

Note: Sensor A, starting composition Ag-AgCl-H_2O; sensor B, starting composition Ag-AgCl-3M HCl. Experimental configuration as in Figure 2.
* Spectrophotometric method (Vernet et al., 1987). MCl^{-} data for internal sensors averaged from two duplicate values.
** A reference experiment at 4 kbar and 700 °C taken from Chou (1978) in Chou (1987). P_{H_2} calculated from Equation 3.33 of Chou (1987).
† Calculated for pure H_2O, see Table 1.
‡ ΔFMQ = log f_{O_2} (column 4) − log f_{O_2} (FMQ), FMQ taken from Hewitt (1978) in Chou (1987).
§ P_{H_2} read at the end of the experiment.

fully tested under various conditions. The main advantage of the new membrane design shown in Figure 2 is that the H_2 diffusing zone is restricted to the isothermal part of the furnace. Therefore, the f_{H_2} recorded by the membrane is that prevailing at the temperature of the reaction chamber. This last point is demonstrated conclusively by the good agreement noted among the P_{H_2} values of the membrane and the sensors placed inside the reaction chamber. This is an important advantage in experimental design when compared with the average P_{H_2}, which would result in long membranes crossing large temperature gradients, as usually employed in IHPV (Webster, personal communication, 1989). Although this new type of membrane consumes a significant percentage of our pressure vessel volume, high performance furnaces can be designed that allow an isothermal zone of about 150 cm^3 (Roux and Lefèvre, 1992) to accommodate samples, Shaw membrane, and thermocouples. Another advantage of the new membrane, compared with other designs (Hewitt, 1978), is that the problem of collapse of the high-pressure capillary is prevented. We found that collapse of the stainless-steel high-pressure capillary is a systematic problem with membranes made following Hewitt (1978) at high T and P ($T > 700$ °C and $P > 4$ kbar), leading to erroneous P_{H_2} values, especially when H_2 transfer occurs from the membrane toward the vessel. Finally, it is worth noting that manufacturing this new type of membrane requires basically the same materials and level of technical ability as the original design does (Shaw, 1963; Piwinskii et al., 1973; Hewitt, 1978; Webster, personal communication, 1989). The new membrane design has been satisfactorily used for up to 45 d at up to 900 °C, total pressure of up to 4.5 kbar, and H_2 pressure of up to 60 bars.

Second, the use of a Au confining cell makes it possible to partially confine H_2 in IHPV by restricting the volume of H_2 diffusion, thus reducing the time of equilibration between vessel and membrane. In addition to allowing the measurement of P_{H_2}, this design opens the new possibility of controlling P_{H_2} by the Shaw membrane in IHPV (i.e., without initially loading the vessel with H_2). Practically, this possibility is limited to the combined use of a confining cell made of Au and of membranes made of metals having high H_2 permeabilities, such as AgPd alloys (see Chou, 1987; Gunter et al., 1987). For use in experiments of long duration, periodic replenishment of the H_2 line [in a way similar to that pioneered by Hewitt (1977, 1978) for CSPV] is probably needed to maintain a constant P_{H_2} inside the cell, although this has not been tested in the present study. It is worth noting that use of this experimental configuration requires the vessel to be operated vertically. Because of the density contrast between H_2 and Ar molecules, horizontal stratification of H_2 and Ar is probably established inside the Au confining cell (and also in all vessels working vertically with H_2-Ar mixtures; Joyce, personal communication, 1989). The magnitude of this effect has not yet been precisely determined (for example with H_2 sensors), but may be important in preventing major loss of H_2 at the bottom of the cell. This phenomenon may be responsible for the difference in P_{H_2} (6 bars, Table 2) between the membrane and the sensors placed inside the confining cell (the high values given by the sensors are in agreement with their position above the membrane, Fig. 2). Alternatively, these sensors may record P_{H_2} values of an earlier osmotic equilibrium state than the membrane, because of the lower permeability constant of Pt compared with AgPd (Gunter et al., 1987). Finally, another important advantage of using the confining cell is to limit the amount of H_2 in direct contact with the autoclave materials, thereby reducing problems due to interaction of H_2 with steels of the autoclave (Seward and Kishima, 1987).

An important conclusion from this paper is the systematic use of calculations to model mass transfers of H_2 and to predict the evolution of P_{H_2} in Shaw membranes and vessels. The general success of our calculations strongly supports the validity of the experimental data base for H_2 permeabilities in both noble metals and steels (Chou, 1986, 1987; Gunter et al., 1987). For CSPV, the difference between calculated and observed P_{H_2} seems to in-

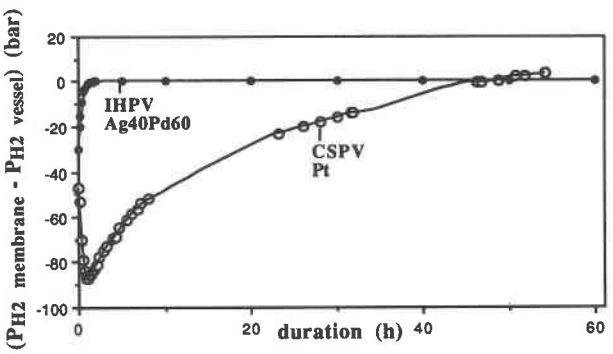

Fig. 8. Value of (P_{H_2} membrane − P_{H_2} vessel) vs. experiment duration illustrating practical problems when using low volume vessels (CSPV) in combination with low permeability membranes (Pt). Experimental conditions for the CSPV as in Figure 3A and text. Note that the H_2 pressures read by the membrane are generally different from those prevailing inside the vessel. In contrast, for an IHPV equipped with an AgPd membrane (experimental conditions as in Fig. 5 and text), osmotic equilibrium is rapidly attained and maintained.

crease with both total pressure and dilution of H_2 by other gases but remains within reasonable values (±1 bar, Fig. 4B, corresponding to ±0.12 log f_{O_2}). On the other hand, more difficulties were encountered when modeling membrane responses in IHPV, mainly because the temperature in the free volume of the vessel is less homogeneous than in CSPV and also because of H_2 loss through the vessel walls. Nevertheless, the calculated P_{H_2} (Fig. 5) are kept in the range of ±8 bars around the measured value, which, for these experimental conditions, corresponds to an error of ±0.18 log f_{O_2}.

Finally, it must be stressed that the volumes of the different H_2 reservoirs (vessel free volume and H_2 line) are critical in determining membrane responses and their practical use. Although hardly mentioned in the literature, this point merits further discussion. In most systems, typical membranes and H_2 line volumes are in the 10 cm³ range, unless transducers are employed (Gunter et al., 1979). On the contrary, vessel free volumes may change by several orders of magnitude from about 1 cm³ (CSPV) to more than 1000 cm³ for some IHPV. As a consequence, the buffering H_2 reservoir may be alternatively the vessel (in the case of IHPV without a confining cell) or the H_2 line (in the case of low volume vessels such as CSPV). This has no practical influence as long as membranes having high permeabilities (typically AgPd) are used, because the osmotic equilibrium between the two reservoirs is rapidly attained (2 h) and maintained, as in the case of an IHPV equipped with an $Ag_{40}Pd_{60}$ membrane (Fig. 8). In contrast, when low permeability membranes (typically Pt) are employed with low-volume vessels, the H_2 pressures read by the membrane are generally different from those prevailing inside the vessel (CSPV with a Pt membrane, Fig. 8). Constraints imposed by the slow kinetics of H_2 equilibration through the membrane lead to an initial stage characterized by much lower P_{H_2} in the membrane than in the vessel (Fig. 8). The time required for attaining osmotic equilibrium is not negligible but is in the same range as the duration of short experiments (2 d, this work, and Hewitt, 1978). Furthermore, equilibrium is not maintained longer than a few hours, and the membrane then reads P_{H_2} higher than inside the vessel, mainly because of the persistent loss of H_2 through the vessel walls (Figs. 3, 8). Differences of a few bars of P_{H_2} may correspond to significant changes in the f_{O_2} conditions, especially at conditions more oxidizing than NNO buffer. For example, at log f_{O_2} = NNO + 1, 600 °C and 1000 bars (which are conditions closely approached in Fig. 4A), an uncertainty of ±1 bar in P_{H_2} would correspond to an error of ±0.4 in log f_{O_2}. Thus, the use of Shaw membranes under these particular conditions (i.e., low-volume vessel and Pt membrane) requires special experimental procedures and care (Hewitt, 1978).

Acknowledgments

We acknowledge the technical assistance of A. Mulot and A. Rouillier in CRPG. D. Hewitt and M. Pownceby provided technical support and information at crucial stages of this study. I.-Ming Chou, J. Clemens, M. Naney, D. Joyce, and J. Webster informed us about various detailed aspects of the use of solid buffers, sensors, membranes, and effects of H_2 on autoclave steels. The Cl analyses were performed by the Laboratoire de Chimie, CRPG. This work was supported by CRPG, CRSCM, and DBT-1990/4.28 and DBT 1991/4.29 and reviewed by H.St.C. O'Neill and M. Pownceby. Special thanks to I.-Ming Chou for his very thorough review. This is DBT-INSU contribution no. 405.

References cited

Burnham, C.W., Holloway, J.R., and Davis, N.F. (1969) Thermodynamic properties of water to 1000 °C and 10000 bars. Geological Society of America Special Paper, 132, 96 p.

Chou, I.-M. (1978) Calibration of oxygen buffers at elevated P and T using the hydrogen fugacity sensor. American Mineralogist, 63, 690–703.

——— (1986) Permeability of precious metals to hydrogen at 2 kb total pressure and elevated temperatures. American Journal of Science, 286, 638–658.

——— (1987) Oxygen buffer and hydrogen sensor technique at elevated pressures and temperatures. In H.L. Barnes and G.C. Ulmer, Eds., Hydrothermal experimental techniques, p. 61–99. Wiley, New York.

Chou, I.-M., and Cygan, G.L. (1989) Equilibrium and steady state redox control in hydrothermal experiments. International Geological Congress Abstracts, 28, 287.

——— (1990) Quantitative redox control and measurement in hydrothermal experiments. In R.J. Spencer and I.-M. Chou, Eds., Fluid-mineral interactions: A tribute to H.P. Eugster, p. 3–15. Lancaster, San Antonio.

Chou, I.-M., and Eugster, G.L. (1976) A sensor for hydrogen fugacities at elevated P and T and applications. Eos, 57, 340.

Eugster, H.P. (1957) Heterogeneous reactions involving oxidation and reduction at high pressures and temperatures. Journal of Chemical Physics, 26, 1760–1761.

——— (1959) Reduction and oxidation in metamorphism. In P.H. Abelson, Ed., Researches in geochemistry, p. 397–426. Wiley, New York.

Frantz, J.D., Ferry, J.M., Popp, R.K., and Hewitt, D.A. (1977) Redesign of the Shaw apparatus for controlled hydrogen fugacity during hydrothermal experimentation. Carnegie Institution of Washington Year Book, 76, 660–662.

Gunter, M.D., Myers, J., and Wood, J.R. (1979) The Shaw bomb, an ideal hydrogen sensor. Contributions to Mineralogy and Petrology, 70, 23–27.

Gunter, M.D., Myers, J., and Girsperberg, S. (1987) Hydrogen: Metal membranes. In H.L. Barnes and G.C. Ulmer, Eds., Hydrothermal experimental techniques, p. 100–120. Wiley, New York.

Hamilton, D.L., Burnham, C.W., and Osborn, E.F. (1964) The solubility of water and effects of oxygen fagacity and water content on crystallisation in mafic magmas. Journal of Petrology, 5, 21–39.

Harvie, C., Weare, J.W., and O'Keefe, M. (1980) Permeation of hydrogen through platinum: A re-evaluation of the data of Chou et al. Geochimica et Cosmochimica Acta, 44, 899–900.

Hewitt, D.A. (1977) Hydrogen fugacities in Shaw bomb experiments. Contributions to Mineralogy and Petrology, 65, 165–169.

——— (1978) A redetermination of the fayalite-magnetite-quartz equilibrium between 650 and 850 °C. American Journal of Science, 278, 715–724.

Holloway, J.R. (1971) Internally heated pressure vessels. In G.C. Ulmer, Ed., Research techniques for high pressure and high temperature, p. 217–258. Springer-Verlag, New York.

Pichavant, M. (1987) Effects of B and H_2O on liquidus phase relations in the haplogranite system at 1 kbar. American Mineralogist, 72, 1056–1070.

Piwinskii, A.J., Weidner, J.R., and Carman, J.H. (1973) An osmotic membrane for hydrogen pressure measurements at elevated temperatures and pressures. Journal of Physics E: Scientific Instruments, 6, 603.

Robie, R.A., Hemingway, B.S., and Fisher, S.R. (1978) Thermodynamic properties of minerals and related substances at 298.15 K and 1 bar (10^5 pascal) pressure and at higher temperatures. U.S. Geological Survey Bulletin 1452, 1–456.

Roux, J., and Lefèvre, A. (1992) A fast quench device for internally heated pressure vessels. European Journal of Mineralogy, in press.

Scaillet, B., Pichavant, M., and Roux, J. (1991) Tourmaline, biotite and muscovite stability in felsic peraluminous liquids. Eos, 72, 311.

Seward, T.M., and Kishima, N. (1987) Problems in working with hydrogen under hydrothermal conditions. In H.L. Barnes and G.C. Ulmer, Eds., Hydrothermal experimental techniques, p. 141–156. Wiley, New York.

Shaw, H.R. (1963) Hydrogen-water vapour mixtures; control of hydrothermal experiments by hydrogen osmosis. Science, 139, 1220–1222.

Shaw, H.R., and Wones, D.R. (1964) Fugacity coefficients for hydrogen gas between 0 and 1000 °C, for pressures to 3000 atm. American Journal of Science, 262, 918–929.

Vernet, M., Marin, L., Boulmier, S., Lhomme, J., and Demange, J.C. (1987) Dosage du fluor et du chlore dans les matériaux géologiques y compris les échantillons hyperalumineux. Analusis, 15, 490–498.

Manuscript received July 8, 1991
Manuscript accepted January 9, 1992